PHYSICAL ELECTRONICS

Application Note

TiN Composition Measurements by Auger Electron Spectroscopy

Titanium nitride (TiN) has many attractive characteristics such as low electrical resistance, good corrosion resistance, considerable hardness and a high melting point. These properties make it a useful material for a wide variety of applications. TiN is commonly used in the semiconductor industry for diffusion barriers and as an adhesion layer.

It is also used as a hard coating for machine tools, and as a protective or decorative coating in many other technical applications. In order to control deposition processes and relate them to material properties, it is useful to characterize the Ti:N composition of the films.

Auger Electron Spectroscopy (AES) is a powerful technique particularly suited for thin film characterization. Unfortunately, the quantification of TiN by AES is a somewhat difficult problem, because the major N $KL_{23}L_{23}$ peak at approximately 389 eV interferes with the Ti $L_3M_{23}M_{23}$ peak at approximately 390 eV.

A variety of solutions,[1-6] of varying rigor and ease-of-use, have been proposed. This publication demonstrates the approach of using a minor N Auger peak, which has no direct overlap with a Ti peak, to determine the N content in TiN.[2] This approach is easily applied to data obtained using a Cylindrical Mirror Analyzer (CMA), as found on the PHI 680 Scanning Auger Nanoprobe™.

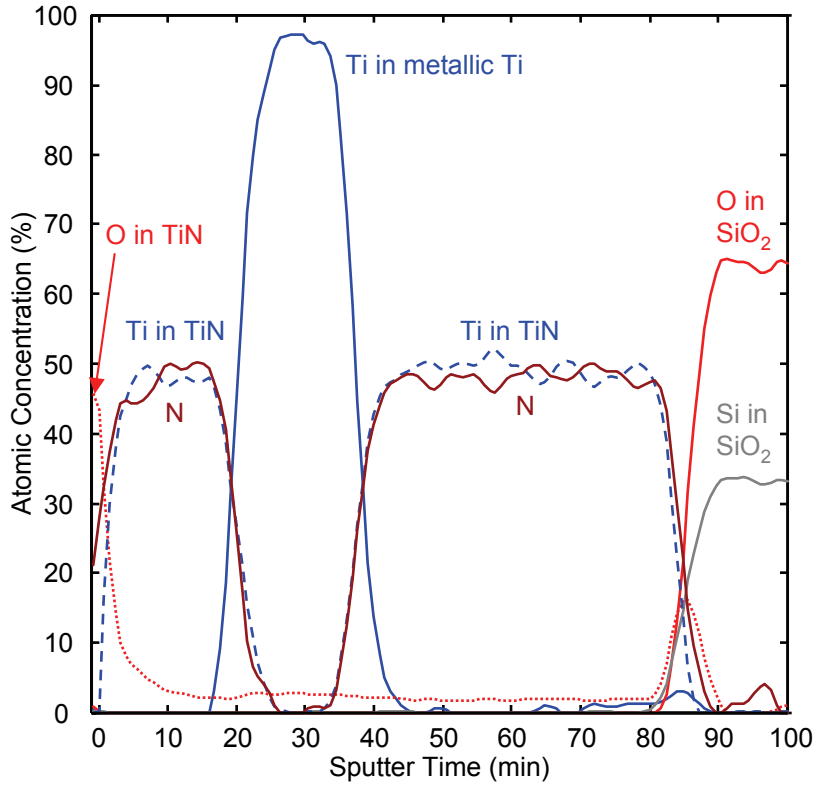

Figure 1. Numerical analysis results for a TiN/Ti/TiN/SiO_2 sputter depth profile were obtained using PHI MultiPak.

1) D.G. Watson, W.F. Stickle, and A.C. Diebold, *Thin Solid Films* **193/194**, 305 (1990).
2) R. Pantel, D. Levy, and D. Nicolas, *J. Vac. Sci. Technol.* A **6**, 2953 (1988).
3) W. Palmer, *Surface Interface Anal.* **13**, 55 (1988).
4) J.L. Vignes, J.P Langeron, G.I. Grigorov, I.N. Martev, and M.V. Stoyanova, *Vacuum* **42**, 151 (1991).
5) J. Haupt, M.A. Baker, M.F. Stroosnijder, and W. Gissler, *Surface Interface Anal.* **22**, 167 (1994).
6) H. Bender, J. Portillo, and W. Vandervorst, *Surface Interface Anal.* **22**, 167 (1989).

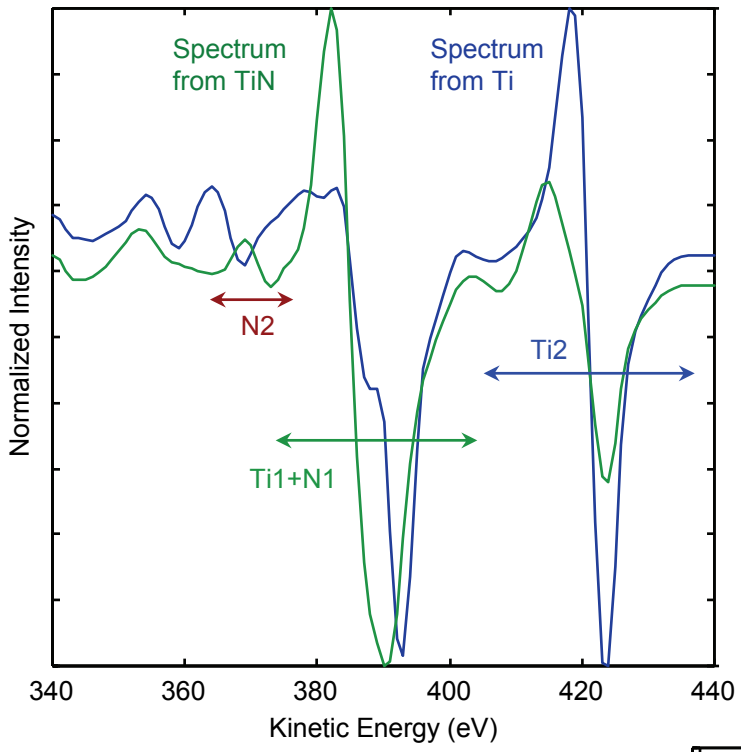

Figure 2. These spectra were extracted from the TiN and Ti layers in the sputter depth profile. The arrows indicate three narrow energy windows to be used for numerical analysis.

The example shown here is TiN/Ti/TiN/SiO_2 on a Si wafer. A sputter depth profile was obtained with the PHI 680 and the data set was reduced using PHI MultiPak™ software. Figure 2 shows the spectra from an acquisition energy window of 340 eV to 440 eV, taken from sputter cycles in the TiN and Ti layers. This energy width encompasses multiple Auger peaks for both N and Ti, including the main N $KL_{23}L_{23}$ (N1) peak at approximately 390 eV, the minor N KL_1L_{23} (N2) peak at approximately 373 eV, the Ti $L_3M_{23}M_{23}$ (Ti1) peak at approximately 390 eV, and the Ti $L_3M_{23}V$ (Ti2) peak at approximately 423 eV.

Figure 3. Peak-to-peak height sputter depth profiles are shown for the three energy windows defined in figure 2, as well as for Si and O.

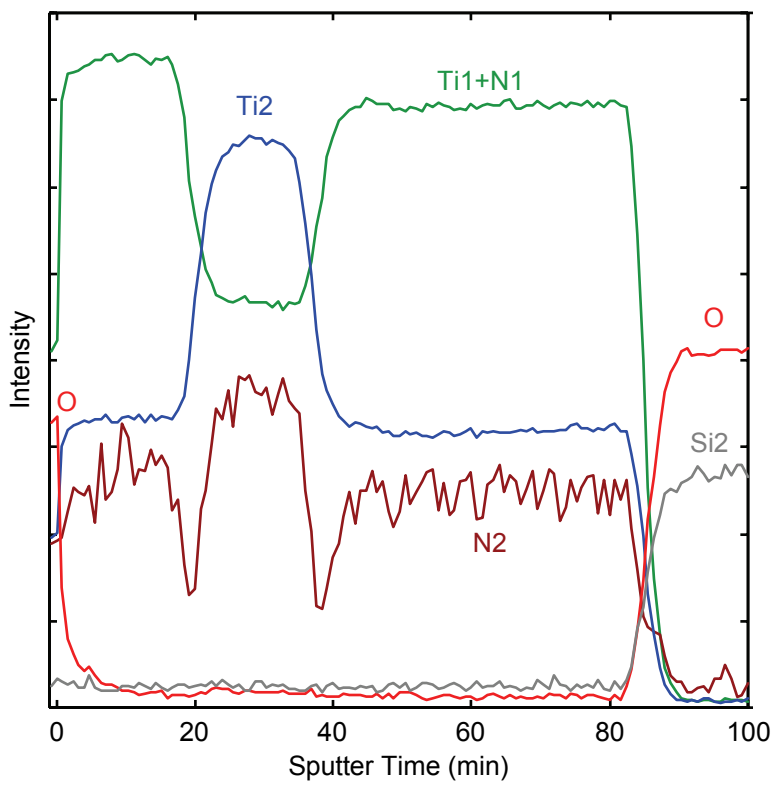

The identification of the peak at 373 eV as a N Auger peak (N $KL_{23}L_{23}$) was made by using the Coghlan and Clausing Auger catalog,[7] and by comparing the peak shape with that of N in TiN, where the N and Ti line shapes in TiN were fully separated using Target Factor Analysis (TFA).[1] The peak position was also consistent with that of N in Co[2] and Hf.[1] After data acquisition, the single energy window was split into narrow energy ranges for N2, N1+Ti1, and Ti2. The resulting peak-to-peak profiles are shown in figure 3, along with the profiles for the Si KLL (Si2) and O KLL peaks.

7) W.A. Coghlan and R.E. Clausing, *Atomic Data* **5**, 317 (1973).

This peak-to-peak height result for N2 does not adequately reject intensity from the nearby Ti interference. Additionally, the Si2 and O profiles suggest that there is slight Si and O throughout the TiN/Ti/TiN layers. Finally, the distinct chemical components present in the sample are not resolved (Ti in TiN is not distinguished from metallic Ti). There are four distinct chemical components in the profile: the surface oxide, TiN, Ti, and SiO_2. Using Linear Least Squares (LLS) fitting, it is possible to chemically resolve these components, reject the noise in the Si and O profiles, and determine a pure nitrogen profile with no Ti interference. The basis spectra for the fitting are extracted from cycles in the profile, where the pure chemical components exist.

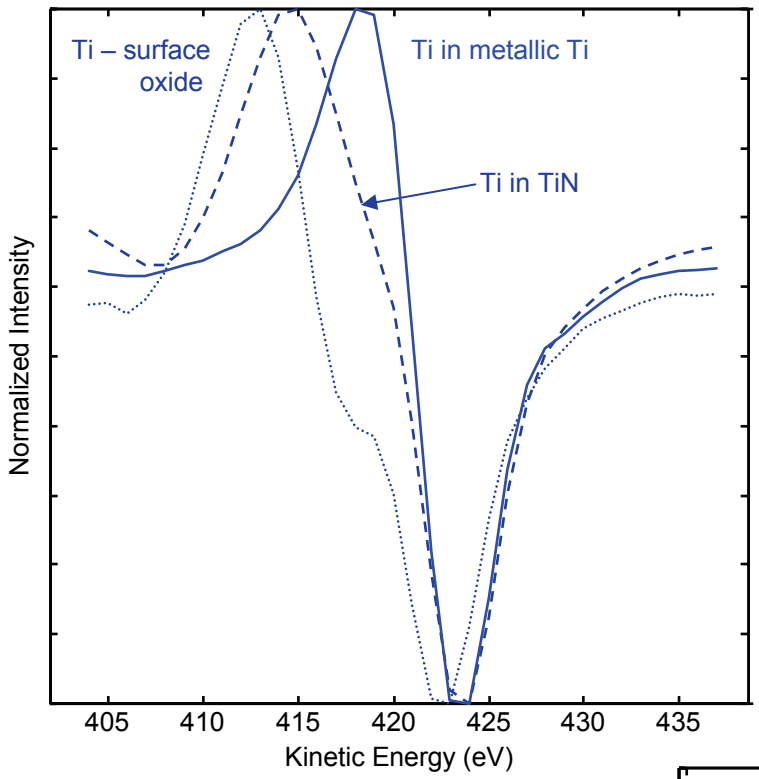

Figure 4. Ti $L_3M_{23}V$ (Ti2) basis spectra are shown for three chemical components.

Figure 5. These intensity depth profiles were acquired for the three Ti chemical components shown in Figure 4.

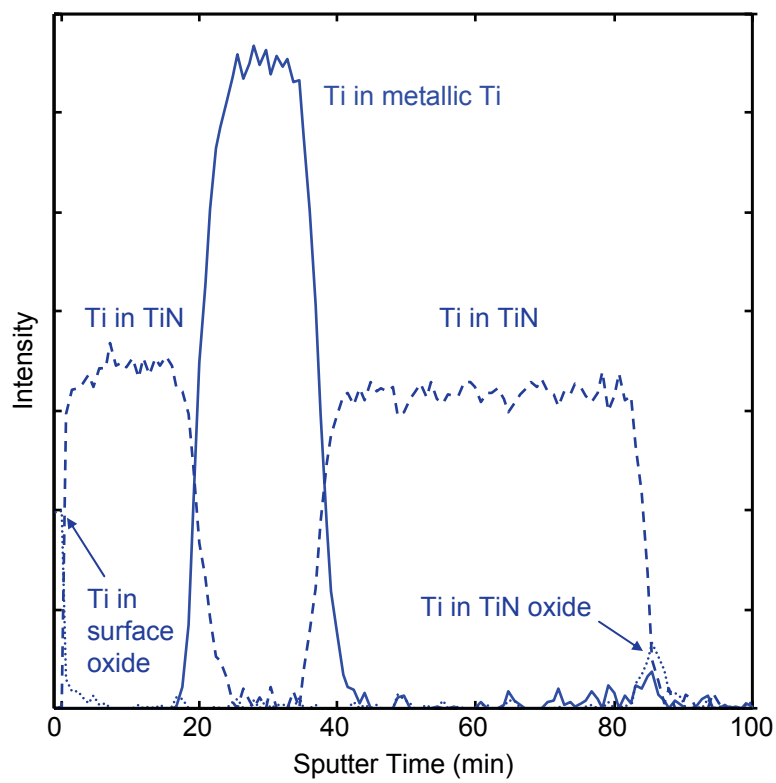

Figure 4 shows the Ti $L_3M_{23}V$ (Ti2) basis spectra for three Ti components: the surface oxide, TiN, and metallic Ti. Figure 5 shows the resulting profiles for these three components. There is no N overlap with this Ti peak, so the intensity profile can be used for Ti quantification.

It is worth noting that the oxidized TiN component appears at the TiN/SiO_2 interface, indicating the formation of a TiN oxide at this interface. This interfacial oxide was not apparent until after LLS fitting.

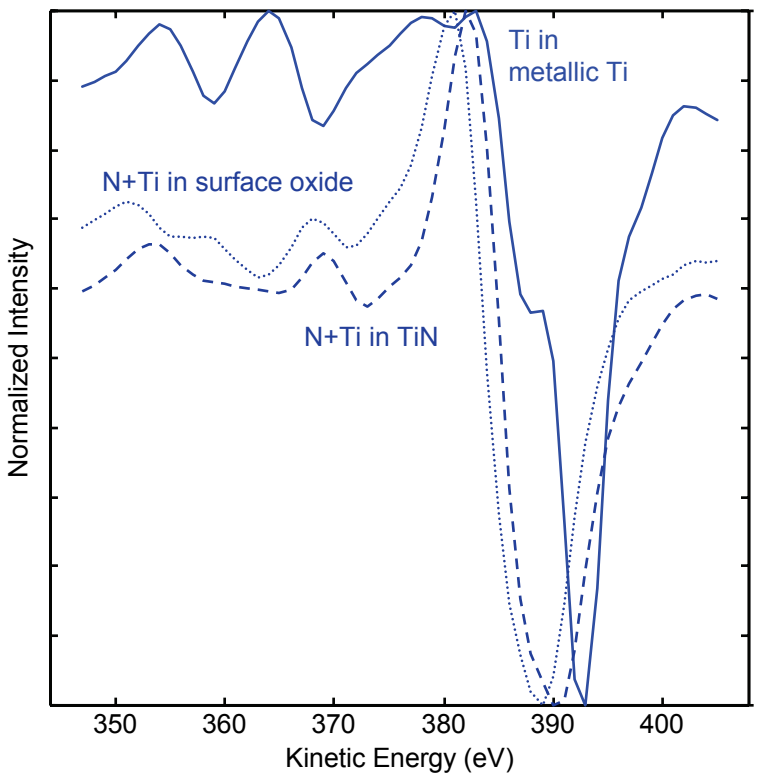

Figure 6. N $KL_{23}L_{23}$ (N1) and Ti $L_3M_{23}M_{23}$ (Ti1) basis spectra are shown for three chemical components.

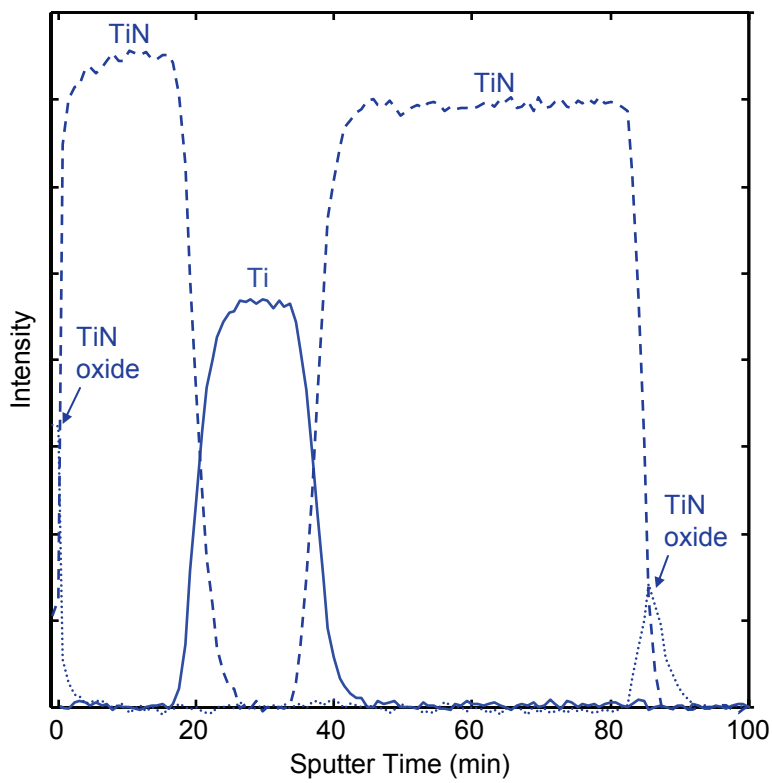

Figure 7. These intensity depth profiles were acquired for the three Ti chemical components shown in Figure 6.

The overlapping N $KL_{23}L_{23}$ (N1) and Ti $L_3M_{23}M_{23}$ (Ti1) peaks can also be used to separate the three Ti chemical components (oxidized TiN, metallic Ti, and TiN), as shown in Figures 6 and 7. However, the intensity in the Ti layer is due only to Ti, while the intensity in the TiN layers is a combination of Ti and N. Therefore, it would not be appropriate to use these profiles for quantification. It is again worth noting that there is a layer of oxidized TiN at the TiN/SiO_2 interface in the oxidized TiN profile.

The minor N KL_1L_{23} (N2) peak can be used to monitor the N intensity. Figure 8 shows the narrow energy window that was defined for this peak. There are two chemical components present within this energy window. The first component is N, whose basis spectrum was taken from a TiN layer. The other component is an interference from a nearby Ti peak structure, whose basis spectrum was taken from the metallic Ti layer. Figure 9 shows the resulting depth profiles for these two components. The N intensity profile has no contribution from Ti and therefore can be used for quantification.

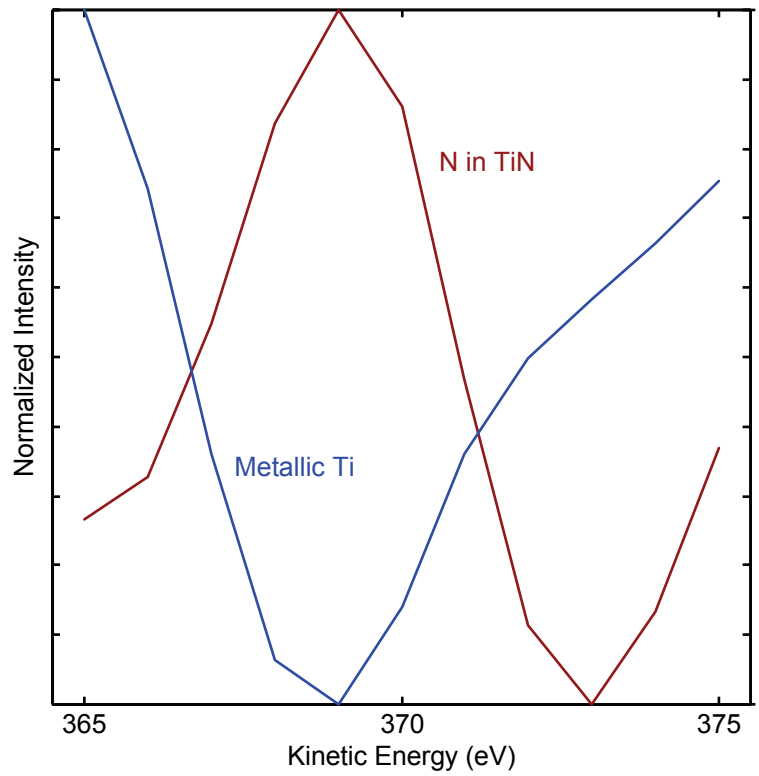

Figure 8. N KL_1L_{23} (N2) and Ti basis spectra are shown for two components, N and Ti.

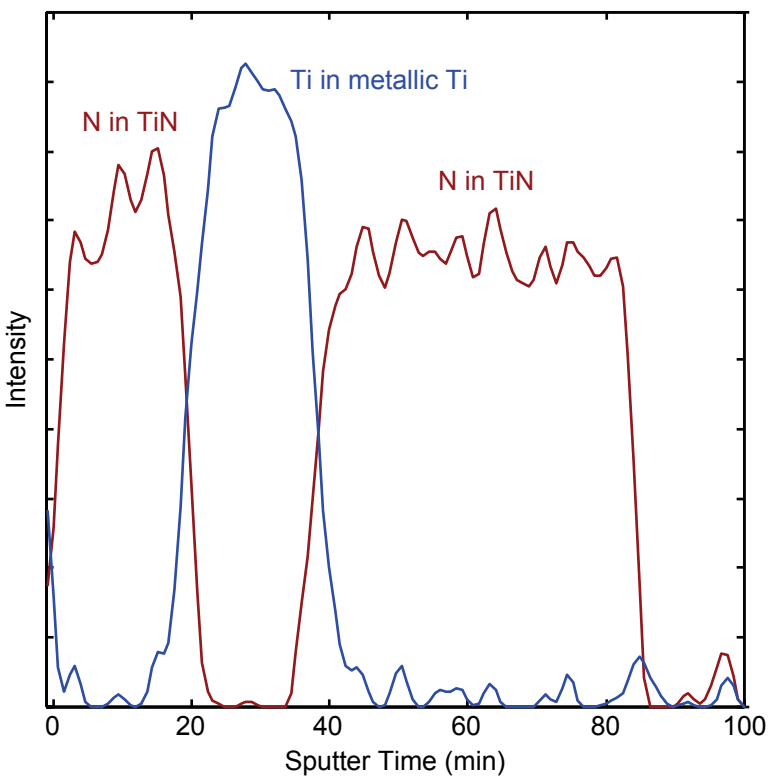

Figure 9. These intensity depth profiles were acquired for the two components shown in Figure 8.

The peak-to-peak Si KLL profile shown in Figure 3 indicates the presence of a low level of Si in the TiN/Ti/TiN layer structure. It is useful to determine whether this is a true Si signal or merely a measure of the peak-to-peak noise in the Si energy window. No recognizable Si peak shape is found in a visual examination of the Si spectra from these cycles.

Linear least squares fitting of the Si spectra with a Si basis spectrum taken from the SiO_2 layer can be used to reject the false Si intensity. Figure 10 shows the Si KLL basis spectrum, and Figure 11 shows a comparison of the original peak-to-peak Si profile with the profile which results from LLS fitting. The LLS results show that there is no Si in the TiN/Ti/TiN layer structure.

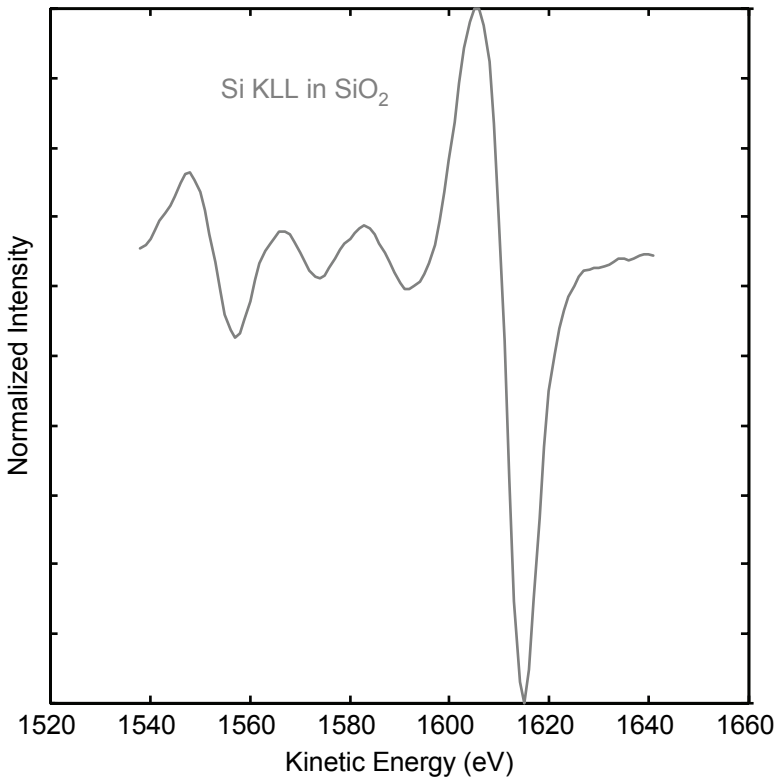

Figure 10. The Si KLL basis spectrum for SiO_2 is shown.

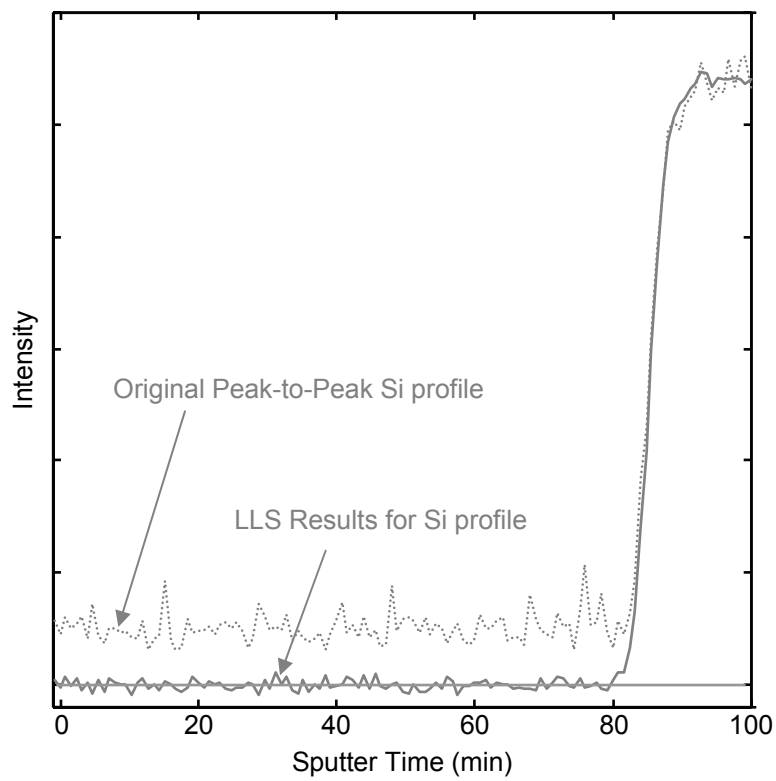

Figure 11. A comparison of the original peak-to-peak Si profile with the Si profile resulting from LLS fitting shows the absence of Si in the TiN/Ti/TiN layer structure.

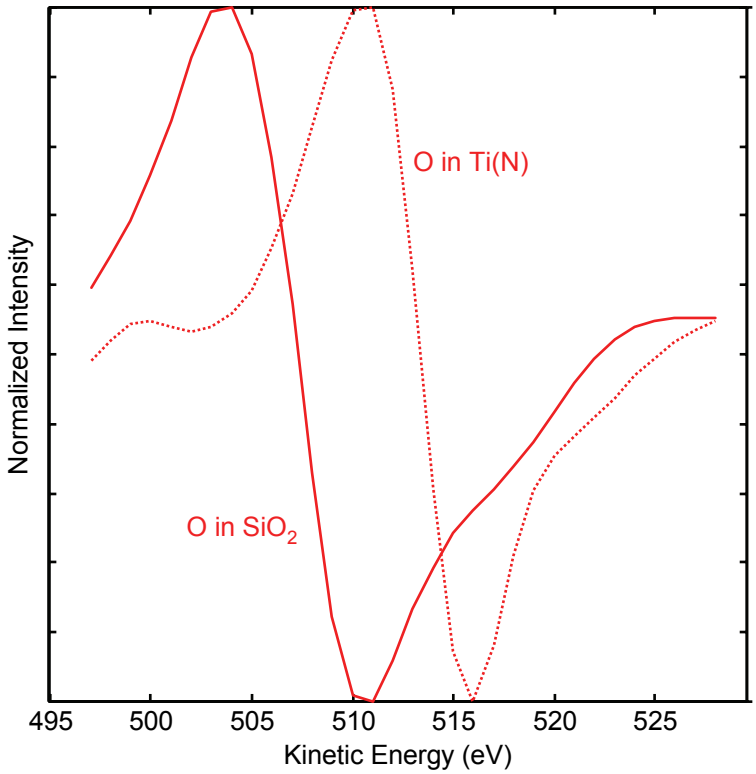

Figure 12. O KLL basis spectra are shown for two chemical environments.

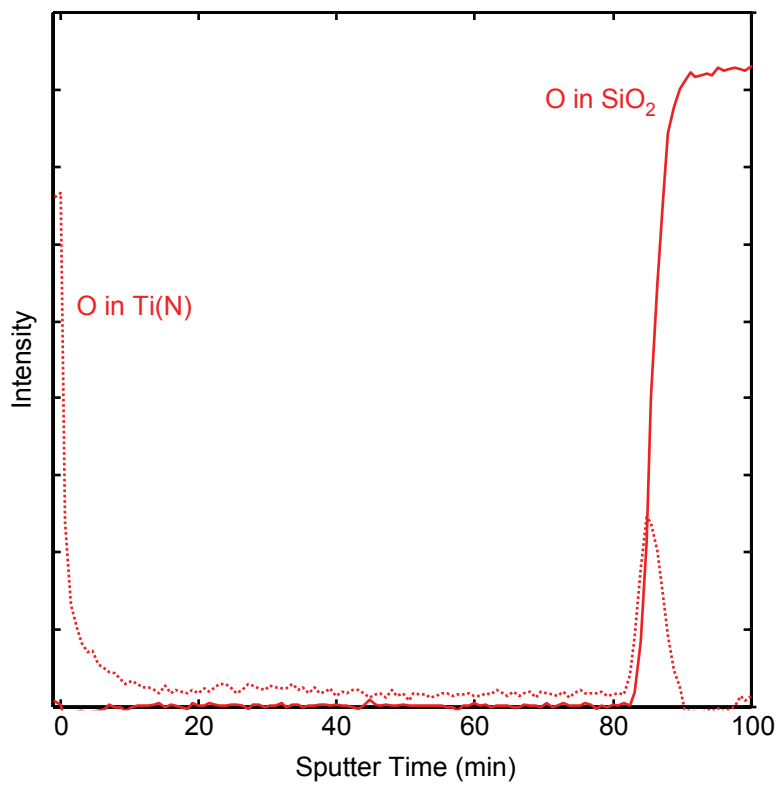

Figure 13. These intensity depth profiles were acquired for the two components shown in Figure 12.

The peak-to-peak O profile shown in Figure 3 indicates the presence of O at a low level in the TiN/Ti/TiN layer structure, as well as O on the TiN surface and at the SiO_2 interface. Figure 12 shows O basis spectra extracted from the SiO_2 layer and from the TiN surface oxide. These two chemical states of O are easily distinguished, and the resulting depth profiles are shown in Figure 13. This figure shows a low level of O through the Ti(N) layers, and a peak in the O in Ti(N) profile at the TiN/SiO_2 interface. This is consistent with the interfacial oxide found for the Ti1 and Ti2 LLS profile results.

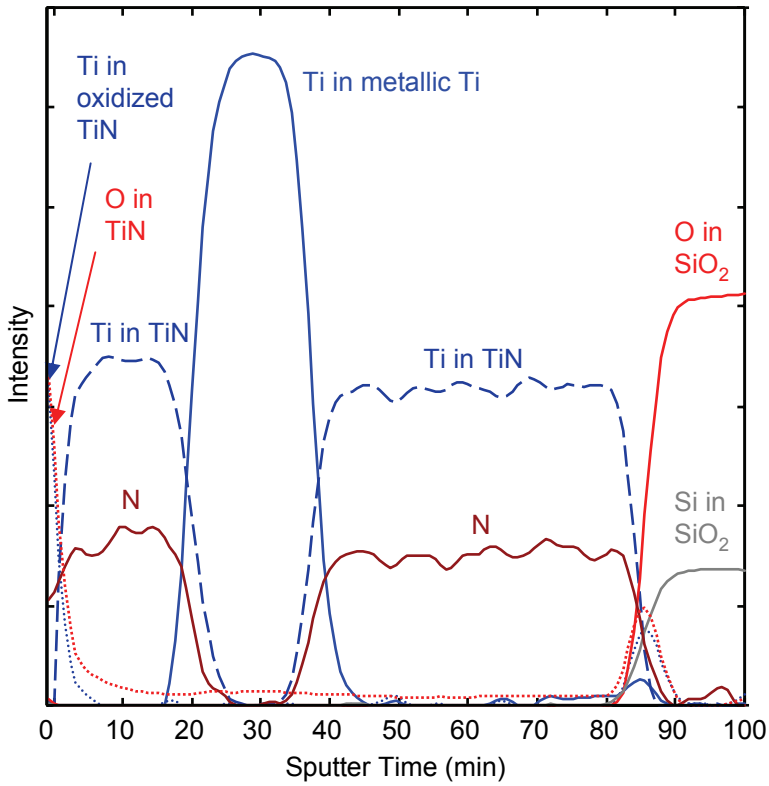

Figure 14. These intensity depth profiles from the LLS analysis show that the various chemical components, as well as Ti and N in TiN, have been separated.

Figure 15. This atomic concentration profile corresponds with the LLS analysis.

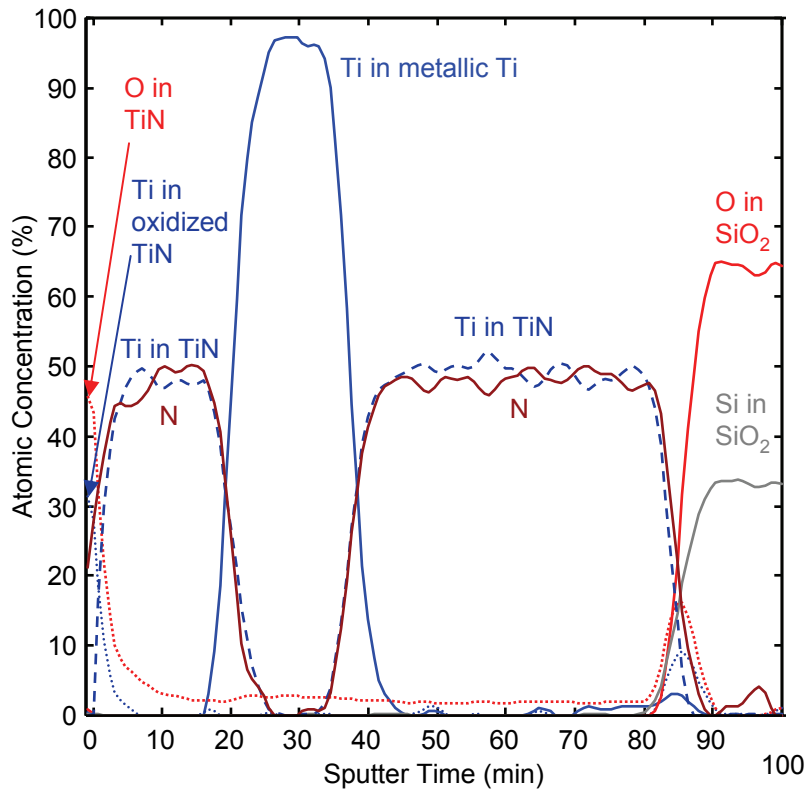

Figure 14 shows the intensity profiles for the three chemical states of Ti (from the Ti2 peak), the two chemical states of O, the LLS fit N2 and the LLS fit Si. Figure 15 shows the corresponding atomic concentration profile, where the N2 sensitivity factor has arbitrarily been set to give nearly stoichiometric TiN. The N2 sensitivity factor can be set using a sample of known Ti:N composition, and that factor can be applied to a sample of unknown composition.

PHYSICAL ELECTRONICS

Physical Electronics USA, 18725 Lake Drive East, Chanhassen, MN 55317
Telephone: 952-828-6200, Website: www.phi.com

ULVAC-PHI, 370 Enzo, Chigasaki City, Kanagawa 253-8522, Japan
Telephone 81-467-85-4220, Website: www.ulvac-phi.co.jp

Physical Electronics GmbH, Fraunhoferstrasse 4, Ismaning 85737, Germany
Telephone: 49-89-96275-0